Load Current Feedforward Control of Boost Converter for Downsizing Output Filter Capacitor

Daisuke Takei*, Hiroshi Fujimoto**, Yoichi Hori***
The University of Tokyo
5-1-5, Kashiwanoha, Kashiwa, Chiba, 227-8561 Japan
Phone: +81-4-7136-3881*, +81-4-7136-4131**, +81-4-7136-3846***
Fax: +81-4-7136-3881*, +81-4-7136-4132**, +81-4-7136-3847***
Email: takei@hflab.k.u-tokyo.ac.jp*, fujimoto@k.u-tokyo.ac.jp**, hori@k.u-tokyo.ac.jp***

***Abstract*—Boost converters are used for high voltage supplying, and they generally have to use large capacitors to suppress output voltage variations. However, this characteristic makes the converter system very large. In this paper, three load current feedforward control methods, which are considered an unstable zero, are proposed for the boost converter. The proposed methods suppress voltage variation compared to feedback control methods and enable the converter to reduce output filter capacitor. Simulations and experiments are conducted to show the effectiveness of the proposed methods.**

I. INTRODUCTION

Boost converters are used to boost output voltage for applications such as electric vehicles and hybrid electric vehicles. In such systems, the size of the output filter capacitor has to be large due to the necessity to reduce voltage variation. Therefore, designing of output filter plays an important role in downsizing of the system.

One of the methods to minimize the size of the output filter capacitor is using control theory. To suppress voltage variation caused by load variation, [1][2]proposed a controller with high response, and the use of small output filter capacitor is achieved[1][2]. There are some approaches to suppress voltage variation with feedback controllers[3][4]. However, these feedback controllers have problems in terms of response speed or switching frequency variation.

In this paper, it is assumed that the inverter is connected to the secondary side of the boost converter. Therefore, the load current of the boost converter is measurable. To suppress voltage variation quickly, it is important to design the load current feedfoward controller. There has been research conducted on load current feedforward control for boost converter[5]–[7]. Generally, a boost converter is a non-minimum phase system[8]. The transfer function from the duty ratio to the output voltage has an unstable zero. Moreover, the transfer function from the duty ratio to the load current also has an unstable zero, as well. Therefore, if a direct inversion of the plant is made, a load current feedforward controller has unstable poles and the controlled system may become unstable.

In [5], current mode control including load current feedforward is described for boost converters with constant power load. In [6], a load current sensor-less feedforward method using digital control is proposed. In these methods, the unstable zero of the plant is not considered. In [7], a feedforward controller design including how to deal with the unstable zero is described, however, it was only considered in the continuous time domain. In addition, these papers did not mention how to design a precise digital feedforward controller. Furthermore, if a digital feedforward controller is designed, future values are needed as references for the controller, but many of the papers did not consider how to design proper input value for the digital feedforward controller.

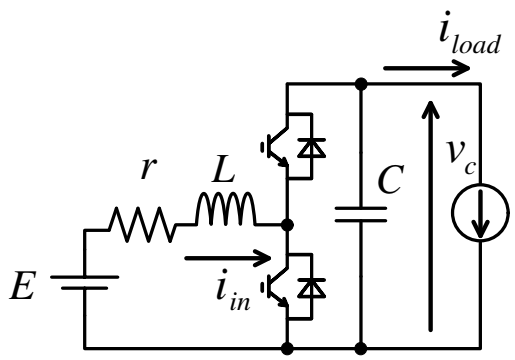

Fig. 1. Configuration of boost converter

In this paper, load current feedforward controllers, which are designed as precise digital controllers, are proposed for a non-minimum phase boost converter. Also, the design method of a proper feedforward controller, which has no delay, is explained. The proposed methods show better voltage variation suppression in comparison to the conventional feedback controller, which achieves downsizing of the output filter capacitor.

II. MODELING OF BOOST CONVERTER

The circuit diagram of the boost converter is shown in Fig. 1, where E is the input voltage, r is the resistance of the reactor coil, L is the inductance of the reactor coil, C is the capacitance, i_{in} is the input current of the converter, v_c is the output voltage , and i_{load} is the load current. In this paper, assuming that the boost converter is operated in a continuous conduction mode. The state space model of the boost converter

is expressed by

$$\frac{d}{dt}\boldsymbol{x}(t) = \boldsymbol{A}(\overline{d}(t))\boldsymbol{x}(t) + \boldsymbol{B}\begin{bmatrix} E \\ i_{load}(t) \end{bmatrix}, \quad (1)$$

$$v_c(t) = \boldsymbol{c}\boldsymbol{x}(t),\ \boldsymbol{x}(t) := [i_{in}(t)\ v_c(t)]^T, \quad (2)$$

$$\left[\begin{array}{c|c} \boldsymbol{A} & \boldsymbol{B} \\ \hline \boldsymbol{c} & \boldsymbol{O} \end{array}\right] := \left[\begin{array}{cc|cc} -\frac{r}{L} & -\frac{\overline{d}(t)}{L} & \frac{1}{L} & 0 \\ \frac{\overline{d}(t)}{C} & 0 & 0 & -\frac{1}{C} \\ \hline 0 & 1 & \multicolumn{2}{c}{\boldsymbol{O}} \end{array}\right],$$

where $d(t)$ is the duty ratio and $\overline{d}(t) := 1-d(t)$. (1) shows that the boost converter is a non-linear system. In order to design a controller, which uses linear control theory, (1) is linearized around an equilibrium point. The state equation of linearized model is given by

$$\frac{d}{dt}\Delta\boldsymbol{x}(t) = \Delta\boldsymbol{A}\Delta\boldsymbol{x}(t) + \Delta\boldsymbol{B}\Delta\boldsymbol{u}(t), \quad (3)$$

$$\Delta v_c(t) = \Delta\boldsymbol{c}\Delta\boldsymbol{x}(t), \quad (4)$$

$$\left[\begin{array}{c|c} \Delta\boldsymbol{A} & \Delta\boldsymbol{B} \\ \hline \Delta\boldsymbol{c} & \boldsymbol{O} \end{array}\right] := \left[\begin{array}{cc|cc} -\frac{r}{L} & -\frac{\overline{D}}{L} & -\frac{V_c}{L} & 0 \\ \frac{\overline{D}}{C} & 0 & \frac{I_{in}}{C} & -\frac{1}{C} \\ \hline 0 & 1 & \multicolumn{2}{c}{\boldsymbol{O}} \end{array}\right],$$

$$\boldsymbol{x}(t) := \boldsymbol{X} + \Delta\boldsymbol{x}(t),\ \Delta\boldsymbol{x}(t) := [\Delta i_{in}(t)\ \Delta v_c(t)]^{\mathrm{T}}, \quad (5)$$

$$\boldsymbol{u}(t) := \boldsymbol{U} + \Delta\boldsymbol{u}(t),\ \Delta\boldsymbol{u}(t) := [\Delta\overline{d}(t)\ \Delta i_{load}(t)]^{\mathrm{T}}, \quad (6)$$

$$\boldsymbol{X} := [I_{in}\ V_c]^{\mathrm{T}}, \boldsymbol{U} := [\overline{D}\ I_{load}]^{\mathrm{T}},$$

$$I_{in} = \frac{I_{load}}{\overline{D}},\ V_c = \frac{E\overline{D} - rI_{load}}{\overline{D}^2}. \quad (7)$$

From (3) and (4), transfer functions from the duty ratio and the load current to the input current and the output voltage of the boost converter are given by

$$\begin{bmatrix} \Delta i_{in}(s) \\ \Delta v_c(s) \end{bmatrix} = \begin{bmatrix} \Delta P_{i1}(s) & \Delta P_{i2}(s) \\ \Delta P_{v1}(s) & \Delta P_{v2}(s) \end{bmatrix} \begin{bmatrix} \Delta\overline{d}(s) \\ \Delta i_{load}(s) \end{bmatrix}, \quad (8)$$

$$\Delta P_{i1}(s) = \frac{b_{i1}s + b_{i0}}{s^2 + a_1 s + a_0},$$

$$\Delta P_{i2}(s) = \frac{c_{i0}}{s^2 + a_1 s + a_0}, \quad (9)$$

$$\Delta P_{v1}(s) = \frac{b_{v1}s + b_{v0}}{s^2 + a_1 s + a_0},$$

$$\Delta P_{v2}(s) = \frac{c_{v1}s + c_{v0}}{s^2 + a_1 s + a_0}, \quad (10)$$

$$a_1 := \frac{r}{L},\ a_0 := \frac{\overline{D}^2}{LC},\ b_{i1} := -\frac{V_c}{L},$$

$$b_{i0} := -\frac{I_{in}\overline{D}}{LC},\ b_{v1} = \frac{I_{in}}{C},\ b_{v0} = \frac{rI_{in} - \overline{D}V_c}{LC},$$

$$c_{i0} := \frac{\overline{D}}{LC},\ c_{v1} := -\frac{1}{C},\ c_{v0} := -\frac{r}{LC}.$$

Note that the zero of $\Delta P_{v1}(s)$ is unstable. The larger the duty ratio and load current are, the slower the unstable zero is. On the other hand, the zero of $\Delta P_{v2}(s)$ is a slow stable zero which is a constant value determined by r and L.

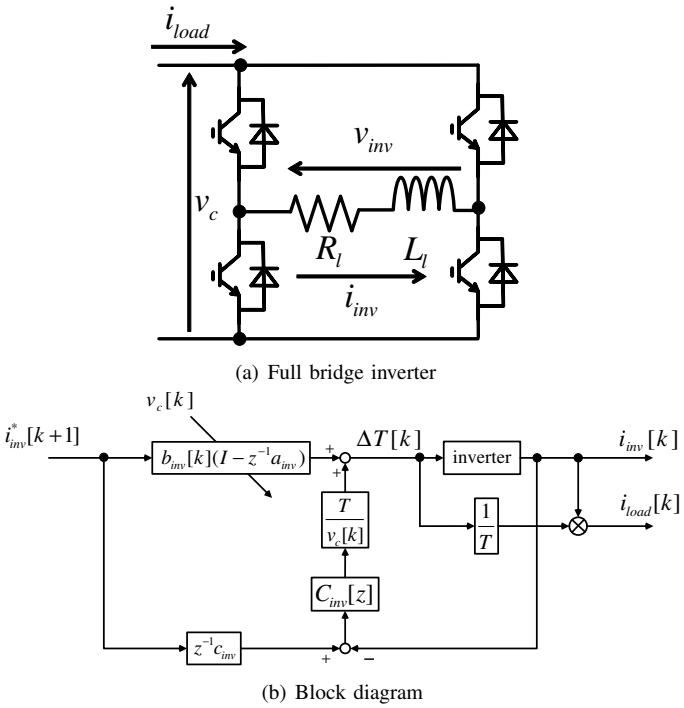

(a) Full bridge inverter

(b) Block diagram

Fig. 2. Single phase inverter model and 2DOF controller

Discretizing (3) and (4) using zero-order hold, the discretized state equation is obtained as

$$\Delta\boldsymbol{x}[k+1] = \Delta\boldsymbol{A}_d\Delta\boldsymbol{x}[k] + \Delta\boldsymbol{B}_d\Delta\boldsymbol{u}[k] \quad (11)$$

$$\Delta v_c[k] = \Delta\boldsymbol{c}_d\Delta\boldsymbol{x}[k], \quad (12)$$

$$\left[\begin{array}{c|c} \Delta\boldsymbol{A}_d & \Delta\boldsymbol{B}_d \\ \hline \Delta\boldsymbol{c}_d & \boldsymbol{O} \end{array}\right] := \left[\begin{array}{c|c} e^{\Delta\boldsymbol{A}T} & \Delta\boldsymbol{A}^{-1}(e^{\Delta\boldsymbol{A}T} - \boldsymbol{I})\Delta\boldsymbol{B} \\ \hline \Delta c & \boldsymbol{O} \end{array}\right] = \left[\begin{array}{cc|cc} \Delta a_{d11} & \Delta a_{d12} & \Delta b_{d11} & \Delta b_{d12} \\ \Delta a_{d21} & \Delta a_{d22} & \Delta b_{d21} & \Delta b_{d22} \\ \hline 0 & 1 & \multicolumn{2}{c}{\boldsymbol{O}} \end{array}\right].$$

III. LOAD CURRENT SIMULATOR

In this paper, arbitrary load variation is generated by a current controller of a full bridge inverter. For example, in the case of a hybrid vehicle system, it is normal for the inverter, which is connected to the secondary side of the boost converter to change current to get any torque, causing voltage variation. Thus, the situation described above is possible in practice. The circuit diagram of a full bridge inverter is shown in Fig. 2(a), where R_l is the load resistance, L_l is the inductance of the load reactance, v_{inv} is the output voltage of inverter, and i_{inv} is the inverter current. The continuous-time state equation of the inverter and the discrete-time state equation using PWM

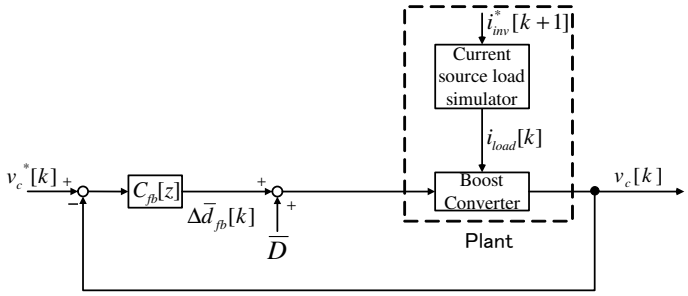

Fig. 3. Voltage control of the conventional method

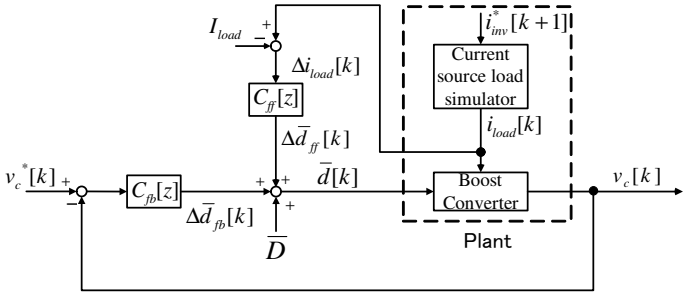

Fig. 4. Voltage control of proposed method 1 and 2

hold are given as [9].

$$\begin{aligned}
\frac{di_{inv}(t)}{dt} &= -\frac{R_l}{L_l}i_{inv}(t) + \frac{1}{L_l}v_{inv}(t), && (13)\\
x_{inv}[k+1] &= a_{inv}x_{inv}[k] + b_{inv}[k]\Delta T[k] && (14)\\
y_{inv}[k] &= c_{inv}x_{inv}[k], && (15)\\
a_{inv} &= e^{-\frac{R_l T}{L_l}},\ b_{inv}[k] = \frac{v_c[k]}{L_l}e^{-\frac{R_l T}{2L_l}},\\
c_{inv} &= 1,\ x_{inv}[k] = i_{inv}[k].
\end{aligned}$$

Note that it is difficult to measure $i_{load}[k]$ due to the carrier ripple. Alternatively, $i_{load}[k]$ is expressed by (16) since $i_{load}[k]$ is equal to average value of $i_{inv}[k]$ during one carrier period T.

$$i_{load}[k] = \frac{\Delta T[k]}{T}i_{inv}[k] \qquad (16)$$

where $i_{inv}[k]$ is controlled with a 2 degree-of-freedom controller shown in Fig. 2(b). The feedforward controller is designed by using single-rate Perfect Tracking Control (PTC) [10]. The continuous-time feedback controller is a PI controller designed with pole-zero cancellation, expressed as

$$C_{inv}(s) = \frac{L_l s + R_l}{\tau_{inv} s},\ \tau_{inv} = 1\ [\text{ms}]. \qquad (17)$$

By discretizing $C_{inv}(s)$ with the Tustin transform method, $C_{inv}[z]$ is obtained.

IV. CONTROL SYSTEM DESIGN

A. Conventional method

The conventional voltage controller shown in Fig. 3 uses a PID controller which is expressed as

$$C_{fb}(s) = K_p + \frac{K_i}{s} + \frac{K_d s}{\tau_{bc}s + 1}. \qquad (18)$$

The conventional controller is designed by pole placement of the fourth root against $\Delta P_{v1}(s)$. By discretizing $C_{fb}(s)$ with the Tustin transform, $C_{fb}[z]$ is obtained.

B. Proposed method 1

The voltage controller of proposed method 1 is designed by using the Zero Phase Error Tracking Control [11] because $\Delta P_{v1}(s)$ is a non-minimum phase system. Block diagram of the proposed method 1 is shown in Fig. 4. From (11) and (12), the discrete-time transfer function from $\Delta\bar{d}[k]$ and $\Delta i_{load}[k]$ to $\Delta v_c[k]$ is obtained by

$$\begin{aligned}
\Delta v_c[k] &= \frac{b_{dv1}z + b_{dv0}}{z^2 + a_{d1}z + a_{d0}}\Delta\bar{d}[k]\\
&+ \frac{c_{dv1}z + c_{dv0}}{z^2 + a_{d1}z + a_{d0}}\Delta i_{load}[k], && (19)\\
a_{d1} &= -(\Delta a_{d11} + \Delta a_{d22}),\\
a_{d0} &= \Delta a_{d11}\Delta a_{d22} - \Delta a_{d12}\Delta a_{d21}, b_{dv1} = \Delta b_{d21},\\
b_{dv0} &= \Delta a_{d21}\Delta b_{d11} - \Delta a_{d11}\Delta b_{d21},\ c_{dv1} = \Delta b_{d22},\\
c_{dv0} &= \Delta a_{d21}\Delta b_{d12} - \Delta a_{d11}\Delta b_{d22}.
\end{aligned}$$

Proposed method 1 controls $\Delta\bar{d}[k]$ to cancel voltage variation caused by $\Delta i_{load}[k]$. Then, from (19) at $\Delta v_c[k] = 0$, the discrete-time transfer function from $\Delta\bar{d}[k]$ to $\Delta i_{load}[k]$ is represented by

$$\Delta P[z] = \frac{\Delta i_{load}[k]}{\Delta\bar{d}[k]} = -\frac{b_{dv1}z + b_{dv0}}{c_{dv1}z + c_{dv0}} = \frac{N[z]}{D[z]}. \qquad (20)$$

and the feedforward controller $C_{ff}[z]$ is given by

$$C_{ff}[z] = \frac{D[z]N[z^{-1}]}{z^2 N^2[1]}. \qquad (21)$$

In proposed method 1, the feedforward controller needs 2 samples before it begins controlling the system.

C. Proposed method 2

Proposed method 2 is designed by PTC which ignores the unstable zero in a continuous time plant [12]. Proposed method 1 is a zero phase error controller but has a magnitude error. In particular, because the unstable zero of the boost converter is far from the pole of the transfer function from $\Delta\bar{d}(s)$ to $\Delta v_c(s)$, its effect of unstable zero is much smaller. Thus, the designed feedforward controller, which ignores the unstable zero, can achieve high tracking performance. Block diagram of the proposed method 2 is same to the proposed method 1.

The transfer function from $\Delta\bar{d}(s)$ and $\Delta i_{load}(s)$ to $\Delta v_c(s)$ is obtained by

$$\begin{aligned}
\Delta v_c(s) &= \frac{b_{v1}s + b_{v0}}{s^2 + a_1 s + a_0}\Delta\bar{d}(s)\\
&+ \frac{c_{v1}s + c_{v0}}{s^2 + a_1 s + a_0}\Delta i_{load}(s). && (22)
\end{aligned}$$

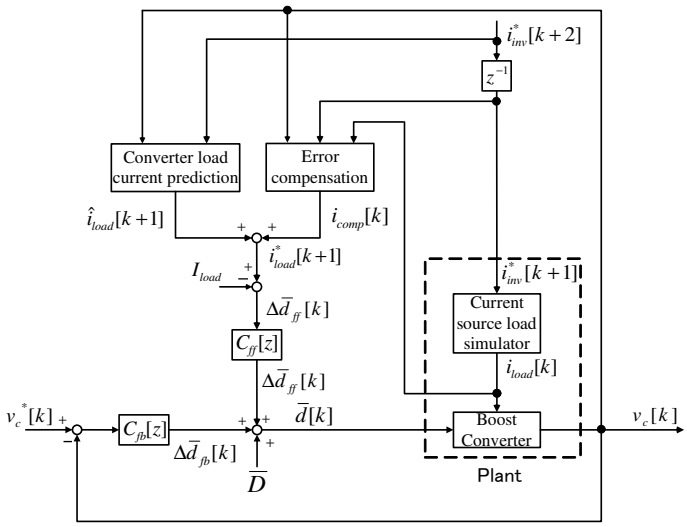

Fig. 5. Voltage control of proposed method 3

$\Delta i_{load}(s)$ of proposed method 2 is calculated in the same way as in proposed method 1. The continuous-time transfer function $\Delta P(s)$ is represented by

$$\begin{aligned}\Delta P(s) &= \frac{\Delta i_{load}(s)}{\Delta\overline{d}(s)} = -\frac{b_{v1}s + b_{v0}}{c_{v1}s + c_{v0}} \\ &= \left(-\frac{b_{v0}}{c_{v1}s + c_{v0}}\right)\left(\frac{b_{v1}}{b_{v0}}s + 1\right), \end{aligned} \tag{23}$$

where $\Delta P(s)$ has an unstable zero. Therefore $\Delta P(s)$ is divided into the minimum phase transfer function $\Delta P_{MP}(s)$ and the non-minimum phase transfer function $n_u(s)$.

$$\Delta P(s) = \Delta P_{MP}(s) n_u(s) \tag{24}$$

$$\Delta P_{MP}(s) = -\frac{b_{v0}}{c_{v1}s + c_{v0}} \tag{25}$$

$$n_u(s) = \frac{b_{v1}}{b_{v0}}s + 1 \tag{26}$$

By discretizing $\Delta P_{MP}(s)$ with carrier period T, the state equations of the feedforward controller are obtained by

$$x_{ptc}[k+1] = a_d x_{ptc}[k] + b_d u_{ptc}[k], \tag{27}$$

$$y_{ptc}[k] = c_d x_{ptc}[k], \tag{28}$$

$$\left[\begin{array}{c|c} a_d & b_d \\ \hline c_d & 0 \end{array}\right] = \left[\begin{array}{c|c} e^{-\frac{c_{v0}}{c_{v1}}T} & -\frac{b_{v0}}{c_{v1}}(e^{-\frac{c_{v0}}{c_{v1}}T} - 1) \\ \hline 1 & 0 \end{array}\right],$$

From (27) and (28), the load current feedforward controller $C_{ptc}[z]$ is given as the following :

$$\Delta\overline{d}_{ff}[k] = C_{ptc}[z]\Delta i_{load}[k+1] \tag{29}$$

$$C_{ptc}[z] = \left[\begin{array}{c|c} O & 1 \\ \hline -\frac{a_d}{b_d} & \frac{1}{b_d} \end{array}\right]$$

In proposed method 2, the feedforward controller needs 1 sample before it begins controlling the system.

D. Proposed method 3

Proposed method 3 uses the predicted value of the load current of the converter, because the load current of the converter is used as the control input of proposed method 1 and 2 is delay. Block diagram of the proposed method 3 is shown in Fig.5. In practice, by delaying the input of the reference torque to the inverter control system by 1 sampling period, the predicted value of the load current is obtained by the feedforward controller of the inverter current. From the reference inverter current after 2 sampling periods, the load current after 1 sampling period $\hat{i}_{load}[k+1]$ is predicted. Here, $v_c[k+1]$ is needed to calculate $\hat{i}_{load}[k+1]$ but $v_c[k+1]$ is 1 sample foregoing value and not able to be measured. When voltage variation after 1 sample is assumed to be sufficiently small, $v_c[k]$ is used in place of $v_c[k+1]$. $\hat{i}_{load}[k+1]$ is thus obtained by

$$\begin{aligned}\hat{i}_{load}[k+1] &= \frac{\Delta T^*[k+1]}{T} i^*_{inv}[k+1] \\ &= \frac{i^*_{inv}[k+1]}{T^2 b_{inv}[k]}(1 - a_{inv}z^{-1}) i^*_{inv}[k+2]. \end{aligned} \tag{30}$$

In practice, the feedforward controller has modeling errors and therefore $\hat{i}_{load}[k+1]$ has errors. The compensation current $i_{comp}[k]$ is defined as $i_{comp}[k] = i_{load}[k] - i^*_{load}[k]$ and the compensated predicted load current of the converter $i^*_{load}[k+1]$ is used for the feedforward control input of the proposed method 3. $i^*_{load}[k+1]$ is calculated by

$$i^*_{load}[k+1] = \hat{i}_{load}[k+1] + i_{comp}[k]. \tag{31}$$

E. Defining equilibrium point

In this paper, the plant model represented by (3) and (4) is a small signal model around an equilibrium point. Therefore, an equilibrium point needs to be defined. In this paper, the equilibrium point is an operating point before the load variation. V_c and I_{load} are the reference voltage $v_c{}^*$ and the load current of the converter before the load variation i^*_{load}. From (7), $\overline{D}$ and I_{in} are calculated. All equilibrium points are described as the following:

$$V_c = v_c^* \tag{32}$$

$$I_{load} = i^*_{load} = \frac{\Delta T^*}{T} i^*_{inv} \tag{33}$$

$$\overline{D} = \frac{E + \sqrt{E^2 - 4rV_cI_{load}}}{2V_c} \tag{34}$$

$$I_{in} = \frac{I_{load}}{\overline{D}} \tag{35}$$

V. SIMULATION

In this section, the effectiveness of the proposed methods is verified by simulation. Parameters of the boost converter are shown in table I. The closed loop pole from v_c^* to v_c is -500 $\mathrm{rad/s}$.

TABLE I
PARAMETERS OF BOOST CONVERTER

DC-bus voltage E	50 V
Output voltage reference v_c^*	100 V
Winding resistance r	113 mΩ
Inductance L	300 μH
Carrier Frequency f_c	10 kHz
Load Inductance L_l	9.35 mH
Load Resistance R_l	7.90 Ω

A. Voltage response against load variation

Simulation results are shown in Fig. 6, where the load variation occurs in the load current simulator at $t = 0$ ms. Large voltage variation occurs with the conventional method after t is 0 ms because the bandwidth of a feedback controller is not high compared to the speed of the load variation. On the other hand, the proposed methods suppress peak voltage variation significantly. The proposed methods 1, 2, and 3 suppress voltage variation about 89.6 %, 93.1 %, and 96.9 % , respectively, compared with the conventional method. In this simulation, the unstable zero before the load variation is a fast zero of 27.7 krad/s. Therefore, there is little impact when the load current feedforward controller ignores the unstable zero as designed in proposed method 2. Thus, proposed method 2 is better than proposed method 1. Furthermore, $i_{load}[k]$ which has a 1-sampling-period delay is used as the input of $C_{ff}[z]$ in proposed methods 1 and 2, while $i^*_{load}[k+1]$ which has no delay is used in proposed method 3. In Fig. 6(d), compensated predicted load current $i^*_{load}[k]$ is the almost same value compared with the measured load current $i_{load}[k]$. Therefore, much further voltage suppression can be achieved.

B. Comparison with different output filter capacitors

Simulation results are shown in Fig. 7, where small output capacitors are used to compare the performances of the control methods. A feedforward controller and a feedback controller are designed against each output capacitor. Since the output filter capacitor is smaller, voltage variation is larger. The proposed methods suppress voltage variation largely compared with the conventional method in each output filter capacitor. By using a load current control, voltage variation is suppressed significantly. As shown by these results, downsizing of the output filter capacitor is achieved.

VI. EXPERIMENT

In this section, the effectiveness of the proposed methods are verified by experiments. Experiments were conducted under the same condition as the simulations.

A. Voltage response against load variation

Experimental results are shown in Fig. 8. In the same way as simulations, large voltage variation occurs when $t = 0$ in the conventional method while in the proposed methods, voltage variations are much smaller. It is assumed that steady state error of the duty ratio between the simulation and the experiment was caused by parameter mismatching.

B. Comparison with different output filter capacitors

Experimental results are shown in Fig. 9. The conventional method allows large voltage variation in small capacitor compared with the proposed methods. On the other hand, the proposed methods suppress voltage variation at almost the same rate of the case when $C = 1600$ μF.

VII. CONCLUSION

In this paper, a precise load current feedforward controller against the load variation of a boost converter was proposed. Simulations and experiments were conducted to show significant suppression effects of the voltage variation. By suppressing voltage variation significantly, smaller output capacitor can be utilized.

In this paper, it was assumed that the unstable zero which the transfer function from the duty ratio to the output voltage is fast because the duty ratio and the load current are very high. Design of feedforward controller when the unstable zero is slow will be considered in the future.

REFERENCES

[1] J. Xu, and Y. Sato: "An investigation of minimum DC-link capacitance in PWM rectifier-inverter systems considering control methods", in Proc. IEEE Energy Conversion Congress and Exposition (ECCE), pp.1071–1077, 2012.

[2] J. Itoh, D. Sato, and T.Shibuya : "Investigation and optimal design of output capacitance in chopper by high speed voltage response control", in Proc. IEEE 15th International Conference on Electrical Machines and Systems (ICEMS), pp.1–6, 2012.

[3] Y. M. Roshan and M. Moallem: "Control of Nonminimum Phase Load Current in a Boost Converter Using Output Redefinition", IEEE Trans. Power Electron., Vol.29, No. 9, pp.5054–5062, 2014.

[4] J. -C. Tsai, C. -L. Chen, Y. -H. Lee, H. -Y. Yang, M. -S. Hsu, and K. -H. Chen: "Modified Hysteretic Current Control (MHCC) for Improving Transient Response of Boost Converter", IEEE Trans. Circuits and Systems, Vol.58, No. 8, pp.1967–1979, 2011.

[5] Y. Li: "Current Mode Control for Boost Converters With Constant Power Loads", IEEE Trans. Circuits and Systems, Vol.59, No. 1, pp.198–206, 2012.

[6] K. Choi, H. -J. Kim, and B. H. Cho: "Load Current-Sensor-Less Feed-Forward Method for Fast Load Transient Response using Digital Control", in Proc. IEEE 28th Annual Applied Power Electronics Conference and Exposition (APEC), pp.2769–2772, 2013.

[7] B. Johansson: "Analysis of DC-DC converters with current-mode control and resistive load when using load current measurements for control", in Proc. IEEE Power Electronics Specialists Conference, pp.165–172, 2002.

[8] Z. Chen, W. Gao, J. Hu, and X. Ye: "Closed-Loop Analysis and Cascade Control of a Nonminimum Phase Boost Converter", IEEE Trans. Power Electron., Vol.26, No.4, pp.1237–1252, 2011.

[9] K. P. Gokhale, A. Kawamura, and R. G. Hoft: "Deat beat microprocessor control of PWM inverter for sinusoidal output wavefortm synthesis", IEEE Trans. Ind. Appl., Vol.23, No. 3, pp.901–910, 1987.

[10] H. Fujimoto, Y. Hori, and A. Kawamura: "Perfect Tracking Control based on Multirate Feedforward Control with Generalized Sampling Periods", IEEE Trans. Ind. Eletron., Vol.48, No.3, pp636–644, 2001.

[11] M. Tomizuka: "Zero Phase Error Tracking Algorithm for Digital Control", Trans. ASME, Jounal of Dynamic Systems, Mesurement, and Control, Vol.109, pp.65–68, 1987.

[12] K. Fukushima, and H. Fujimoto: "Vibration Suppression PTC of Hard Disk Drives with Multirate Feedback Control", Proc. 26th American Control Conference, pp.55–60, 2007.

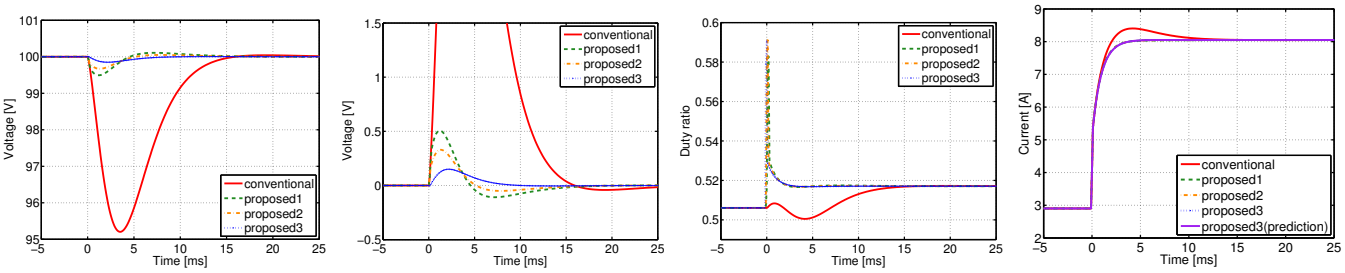

(a) Output Voltage (b) Voltage Error (c) Duty ratio (d) Converter load current

Fig. 6. Simulation results of voltage variation suppression against load variation ($C = 1600\ \mu$F)

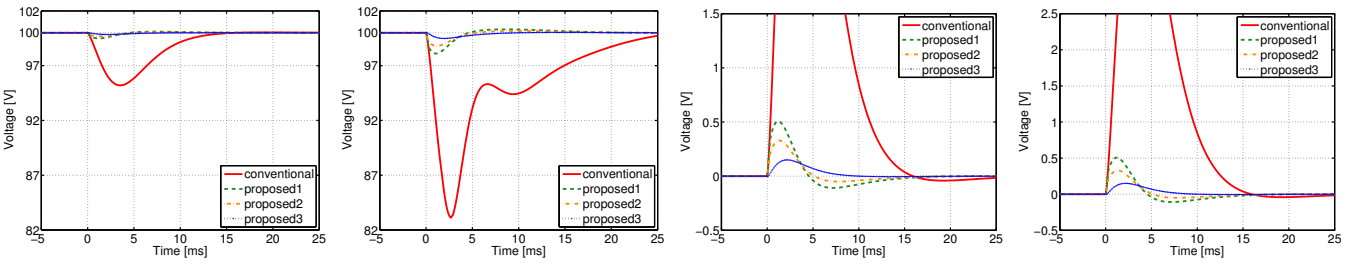

(a) Output Voltage ($C = 1600\ \mu$F) (b) Output Voltage ($C = 400\ \mu$F) (c) Voltage Error ($C = 1600\ \mu$F) (d) Voltage Error ($C = 400\ \mu$F)

Fig. 7. Simulation results of voltage variation suppression when small output filter capacitor is used

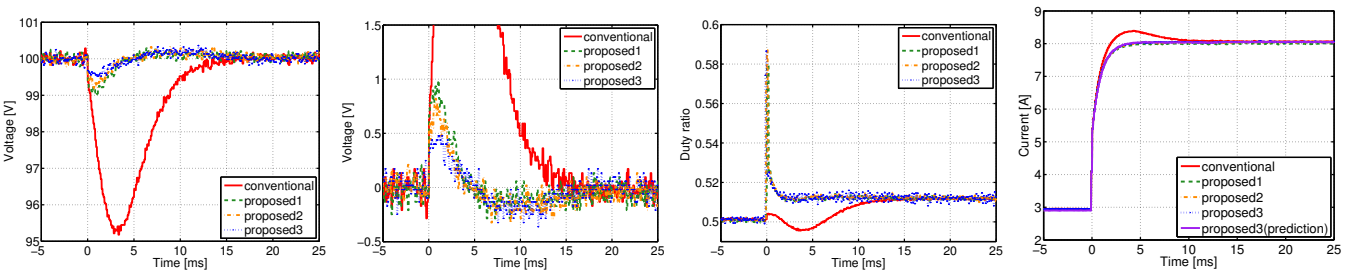

(a) Output Voltage (b) Voltage Error (c) Duty ratio (d) Converter load current

Fig. 8. Experiment results of voltage variation suppression against load variation ($C = 1600\ \mu$F)

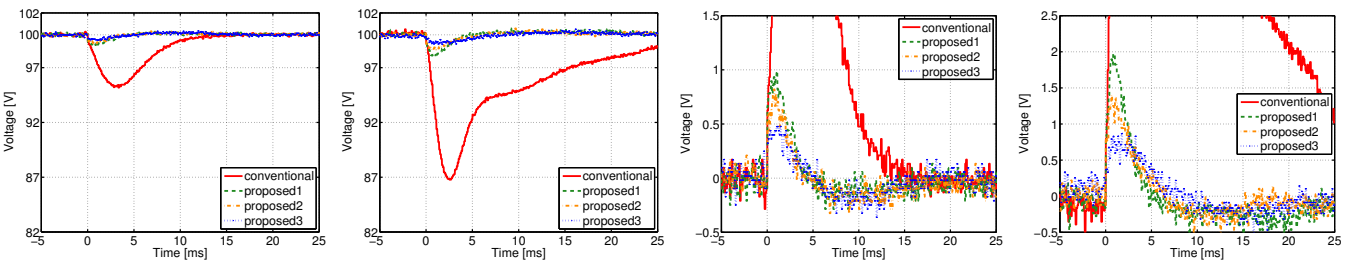

(a) Output Voltage ($C = 1600\ \mu$F) (b) Output Voltage ($C = 400\ \mu$F) (c) Voltage Error ($C = 1600\ \mu$F) (d) Voltage Error ($C = 400\ \mu$F)

Fig. 9. Experiment results of voltage variation suppression when small output filter capacitor is used